

AD-A055 180

AIR FORCE INST OF TECH WRIGHT-PATTERSON AFB OHIO SCH--ETC F/G 20/5  
OUTPUT POWER VARIATIONS IN Nd:YAG LASER HOSTS.(U)  
DEC 76 W B MAUPIN

UNCLASSIFIED

AFIT/6EP/PH/76-8

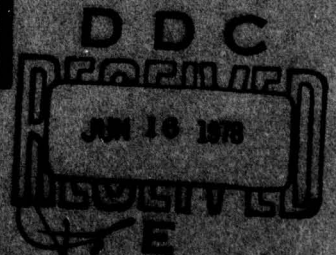
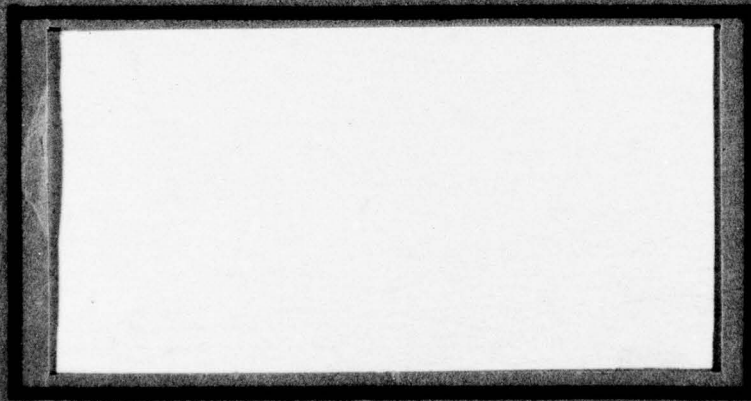
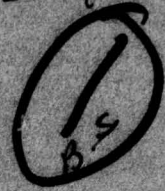
NL




MICROCOPY RESOLUTION TEST CHART  
 NATIONAL BUREAU OF STANDARDS-1963-A

AD A 055180

FOR FURTHER TRAN *A.L.W.*



AD No. \_\_\_\_\_  
DDC FILE COPY

UNITED STATES AIR FORCE  
AIR UNIVERSITY  
AIR FORCE INSTITUTE OF TECHNOLOGY  
Wright-Patterson Air Force Base, Ohio

48 06 18 170

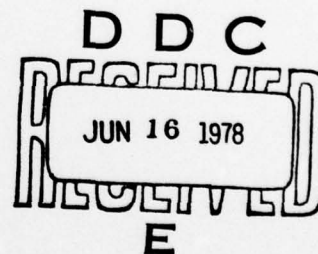
GEP/PH/76-8

OUTPUT POWER VARIATIONS IN  
ND:YAG LASER HOSTS

THESIS

GEP/PH/76-8

Warren B. Maupin, II  
Captain USAF



Approved for public release; distribution unlimited

78 06 13 170

⑭ AFIT/GEP/PH/76-8

⑥ OUTPUT POWER VARIATIONS IN  
ND:YAG LASER HOSTS.

⑨ Master's thesis

THESIS

Presented to the Faculty of the School of Engineering  
of the Air Force Institute of Technology  
Air University  
in Partial Fulfillment of the  
Requirements for the Degree of  
Master of Science

⑬ 68 p.

⑩ by  
Warren B. Maupin, II B. S.  
Captain USAF  
Graduate Engineering Physics

⑪ December 1976

Approved for public release; distribution unlimited.

022 225

elt

Preface

As is the case in any scientific endeavor, the end result of this investigation reflects not only the efforts of the author, but many others. While it is not possible to name all those who have provided guidance, assistance, and encouragement; a few persons deserve special thanks.

The author wishes to thank Captain C. J. Kennedy of SAMSO for proposing and sponsoring this investigation. The assistance of Dr. T. E. Luke during the investigative and reporting stages of this study was invaluable and is deeply appreciated.

Finally, the author is especially grateful to his wife for her patience, understanding, and encouragement.

Warren B. Maupin, II

ACCESSION for		
NTIS	White Section	<input checked="" type="checkbox"/>
DDC	Buff Section	<input type="checkbox"/>
UNANNOUNCED		<input type="checkbox"/>
JUSTIFICATION.....		
.....		
BY.....		
DISTRIBUTION/AVAILABILITY CODES		
Dist. AVAIL. and/or SPECIAL		
A		

## Contents

Preface . . . . .	ii
List of Figures . . . . .	v
Abstract . . . . .	vi
I. Introduction . . . . .	1
II. The Chemistry and Crystal Growth of Nd:YAG . . . . .	3
The Chemistry of Nd:YAG . . . . .	3
The Crystal Growth of Nd:YAG . . . . .	4
Core Effect . . . . .	5
Strain . . . . .	5
Melt Enrichment . . . . .	6
III. Spectroscopy of Nd:YAG . . . . .	9
Absorption and Emission in Nd:YAG . . . . .	9
Fundamental Spectroscopic Parameters . . . . .	11
Lineshape . . . . .	12
Lifetimes . . . . .	12
Cross Sections . . . . .	14
Branching Ratios . . . . .	17
Quantum Efficiency . . . . .	20
Spectroscopic Parameters of Nd:YAG . . . . .	21
IV. Power Output from Nd:YAG Lasers . . . . .	23
Nd:YAG as a Four Level Laser . . . . .	23
The Gain Coefficient . . . . .	24
Gain Saturation in a Homogeneously Broadened Laser Medium . . . . .	26
Laser Oscillation . . . . .	29
Power Output for CW Operation . . . . .	30
Energy Output for Q-Switch Operation . . . . .	32
Key Host Parameters . . . . .	36
V. Energy Transfer Mechanisms . . . . .	38
Resonant Transfer . . . . .	38
Radiation Trapping . . . . .	40
Cross Relaxation . . . . .	40
Multiphonon Nonradiative Decay . . . . .	42
Excited State Pumping . . . . .	43
Auger Recombination . . . . .	44
VI. Recommendations for Future Investigations . . . . .	45

Bibliography . . . . .	49
Appendix A: Supplementary Bibliography . . . . .	52
Vita . . . . .	54

List of Figures

<u>Figure</u>		<u>Page</u>
1	Strain Planes in Nd:YAG . . . . .	6
2	Impurity Concentration Profile for Normal Freezing . . . . .	7
3	Energy Levels in Nd:YAG . . . . .	10
4	Schematic of a Four Level Laser Medium . . . . .	24
5	A Simple Laser Resonator . . . . .	29
6	Energy Transfer Mechanisms . . . . .	39

Abstract

Seemingly identical Nd:YAG laser rods often exhibit significant variations in output power. The purpose of this report is to investigate the possible cause or causes for the performance variations in Nd:YAG laser rods.

The fundamental chemical and crystal growth characteristics of Nd:YAG are reviewed. The spectroscopy of Nd:YAG is discussed with emphasis on the laser transition. The more common spectroscopic parameters are defined and the important relationships between them derived. Expressions relating the laser performance of CW and Q-switched systems to the host parameters are developed and the important parameters ( $n$ ,  $\Delta n$ ,  $\tau_f$ ,  $\tau_{sp}$ ,  $\alpha$ ) are discussed. Possible energy transfer mechanisms to account for performance variations are presented and evaluated.

It is proposed that concentration variations are primarily responsible for laser performance fluctuations and a method for obtaining experimental verification is outlined.

# OUTPUT POWER VARIATIONS

IN

ND:YAG LASER HOSTS

## I. Introduction

In 1958, Schawlow and Townes first proposed the laser (Ref 1). In 1960, Maiman demonstrated the first successful laser system employing a ruby crystal in the pulsed mode of operation (Ref 2). Following the success of Maiman, laser action was achieved using a wide variety of active ions and host materials.

In 1961, Johnson and Nassau (Ref 3) obtained laser action from neodymium (Nd) in calcium tungstate ( $\text{CaWO}_4$ ) and Snitzer (Ref 4) observed lasing from neodymium-doped glass. Over the next few years, neodymium was lased in numerous host materials. Then, in 1964, Guesic, et al., (Ref 5) demonstrated laser action in neodymium-doped yttrium aluminum garnet (Nd:YAG). In the years since its initial discovery, Nd:YAG has emerged as one of the more popular solid state laser materials (Ref 6:44).

However, Nd:YAG is not without its drawbacks. When operated at high continuous wave (CW) powers, thermally induced focusing and birefringence effects produce decreased polarized and  $\text{TEM}_{00}$  power outputs (Ref 7,8). For neodymium concentrations in excess of 1.2 atom percent, the fluorescent lifetime decreases rapidly resulting in increased threshold

pumping requirements (Ref 9:205). The above problems represent limitations on the operation of Nd:YAG laser systems. However, even if a Nd:YAG system is operated within these limitations, another problem exists: seemingly identical laser rods will often exhibit significant variations in power output. The cause(s) of these power variations is not known.

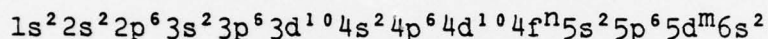
Thus, the primary purposes of this investigation are to propose possible mechanisms for the observed power variations among Nd:YAG laser rods and future areas of investigation to aid in determining the mechanism(s) responsible for those variations. Additionally, it is hoped that this thesis will serve as an introductory source document for those interested in Nd:YAG materials research.

In order to accomplish the above, the chemistry and crystal growth of Nd:YAG are discussed briefly in Chapter II. Then, in Chapter III, the spectroscopy of Nd:YAG is discussed along with the fundamental spectroscopic parameters and how they are determined. In Chapter IV, the important equations for the four level laser are developed and the key host parameters identified. Possible mechanisms for power variations are presented in Chapter V. Recommended areas for future investigations are discussed in Chapter VI. A supplementary bibliography, for those interested in more detailed discussions of the topics covered in this thesis, is presented in Appendix A.

## II. The Chemistry and Crystal Growth of Nd:YAG

### The Chemistry of Nd:YAG

Neodymium is a part of the lanthanide series of elements which are more commonly referred to as the rare-earths. The rare-earth atoms have electronic configurations given by:



where  $m=0,1$  and  $n=0,2,3,\dots,14$ . They are primarily trivalent, although some of the atoms may also be divalent or tetravalent (Ref 10:15). In the trivalent form, the electronic configuration is that shown above except that the  $5d^m$  and  $6s^2$  electrons are missing. Thus, the outermost electrons ( $5s^2 5p^6$ ) comprise the xenon rare-gas shell and are optically inactive. Inside the xenon shell lies the  $4f^n$  shell with its  $n$  optically active electrons ( $n=0,1,\dots,14$ ). Since the  $4f$  shell lies inside the xenon shell, its electrons interact weakly with other ions resulting in sharp spectral lines, high fluorescent yields, and remarkably similar absorption and emission spectra for a given ion in various hosts (Ref 11:267). The neodymium atom (atomic number=60, atomic weight=144.24) corresponds to the  $m=0, n=4$  electronic configuration, while, for the trivalent neodymium ion,  $n=3$ .

Yttrium aluminum garnet has the molecular formula,  $Y_3Al_5O_{12}$ , with molecular weight, 593.7. The overall crystal structure exhibits cubic symmetry with eight molecules per unit cell and a cube edge dimension of 12 angstroms (Ref 12:87).

Because of its cubic symmetry, YAG exhibits isotropic thermal and optical behavior. YAG has a high coefficient of thermal conductivity and a low thermal expansion coefficient, both of which are highly desirable in a laser host. Additionally, YAG is very hard which allows it to be machined, polished and handled without fear of fracture (Ref 9:202).

When YAG is doped with neodymium, the neodymium ions replace the yttrium ions in the garnet structure resulting in a molecular formula of  $Y_{3-x}Nd_xAl_5O_{12}$ , where x represents the number of yttrium ions replaced by neodymium. For example, if the neodymium concentration is one atom percent,  $x=0.03$  (Ref 13). For normal neodymium concentrations (1.0-1.2 atom percent), the properties of Nd:YAG are essentially unchanged from those of pure YAG. Excellent summaries of the important properties of YAG and Nd:YAG may be found in Ref 6 and Ref 12:88-92.

#### The Crystal Growth of Nd:YAG

Although Nd:YAG crystals have been grown by several different methods, the preferred growth technique is Czochralski pulling. Crystals are grown by this method by dipping a rotating seed crystal into a crucible of molten material and withdrawing it at a constant rate. The growth of Nd:YAG requires the use of an iridium crucible due to the high melting point (1970 °C) of Nd:YAG. Use of the iridium crucible requires that the growth process be conducted in an inert atmosphere (typically argon and nitrogen) to avoid oxidation of the crucible and subsequent contamination of the melt (Ref 12:85). The

seed crystal is normally rotated at 40-50 rpm and withdrawal rates usually range from 0.1 to 1.5 mm/hr depending on the dopant level and crystal (or boule) diameter. The growth of high quality Nd:YAG requires that the starting oxides ( $Y_2O_3$ ,  $Al_2O_3$ ,  $Nd_2O_3$ ) used in the melt be dry and of 99.999 percent purity (Ref 9:203). It is also important that the boule diameter and the shape of the boule-melt interface be rigidly controlled (Ref 14:269).

Even under optimum growth conditions, Nd:YAG boules exhibit some undesirable growth characteristics. Three of these, core effect, strain, and melt enrichment are important in the production of laser rods and are discussed below.

Core Effect. During Czochralski growth, facets form at the crystal interface along either the {211} or {110} planes depending on the growth direction. The net effect of these facets is to produce an optically inhomogeneous core that runs the length of the boule and is unsuitable for laser rods. Although this phenomena is well known, the exact cause is not. One proposal is that it is due to a difference in the impurity segregation on the planar faceted and non-faceted interfaces (Ref 9:203). While the core diameter (1-2 mm) appears to be independent of the boule diameter (Ref 14:269), it does vary with growth direction with the smallest core resulting from growth in the  $\langle 111 \rangle$  direction (Ref 9:204).

Strain. Boules grown in the  $\langle 111 \rangle$  direction have a roughly hexagonal cross section due to the faceting of the {211} planes. When the boule is viewed in a Twyman-Green

interferometer, areas of high strain corresponding to the facet boundaries are quite evident as illustrated in Fig. 1. It is

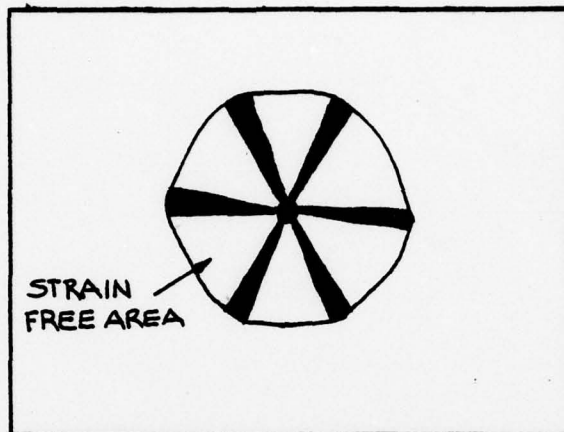


Fig. 1. Strain Planes in Nd:YAG  
(after Ref 14:269)

important that laser rods be cut only from the strain free areas of the boule.

Melt Enrichment. Since the neodymium ion is larger than the yttrium ion it replaces, neodymium tends to be retained in the melt. A measure of this tendency is given by the initial distribution coefficient,  $k_1$ , defined by

$$k_1 = C_s / C_o \quad (1)$$

where  $C_s$  is the initial Nd concentration in the crystal, and  $C_o$  is the initial Nd concentration in the melt. For Nd:YAG, the value of  $k_1$  ranges from 0.12 (Ref 14:269) to 0.21 (Ref 15). Thus, as the boule is pulled from the melt, the concentration of neodymium in the melt increases and the melt is said to be enriched. The increased neodymium concentration in the melt leads to an increase in the neodymium concentration in the boule as it is pulled from the melt. The resulting concentration gradient can be predicted by the normal freezing equation:

$$C_{\ell} = C_0 k_1 (1-g)^{k_1-1} \quad (2)$$

where  $C_{\ell}$  = Nd concentration in the boules at length  $\ell$

$C_0$  = initial Nd concentration in the melt

$k_1$  = initial distribution coefficient

$g$  = fraction of the melt pulled corresponding to length  $\ell$ .

Figure 2 shows the variation of  $C_{\ell}$  as a function of  $g$ .

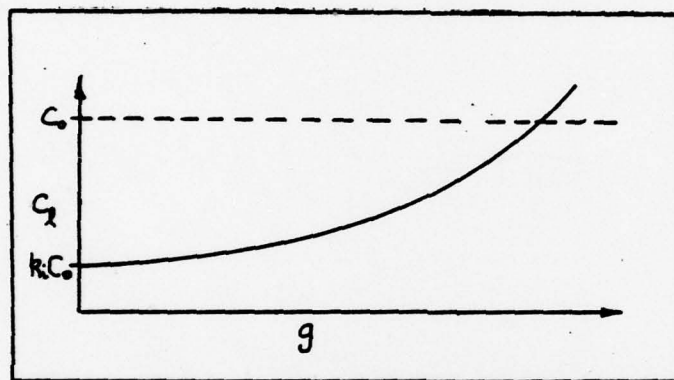


Fig. 2. Impurity Concentration Profile for Normal Freezing (after Ref 16:222)

Experiments by Belt, et al., have confirmed the validity of equation (2) for Nd:YAG. Increases of 20-30 percent in neodymium concentration along the length of a 20 cm boules are typical. Thus, for one atom percent initial neodymium concentration, end to end variations along a 30-50 mm rod are on the order of 0.05-0.10 atom percent and the maximum rod to rod variations among rods from the same boules are 0.10-0.15 atom percent (Ref 14:269-270).

Melt enrichment places serious limitations on the amount of material that can be crystallized from the melt. For example, if the initial neodymium concentration in the boules is one atom percent, when 20 percent of the melt has been crys-

talized the concentration in the boule has increased to approximately 1.2 atom percent - the threshold for concentration quenching. When 40 percent of the melt has been crystalized, the boule concentration has increased to roughly 1.5 atom percent and the growth of high optical quality Nd:YAG becomes extremely difficult (Ref 9:205). Thus, for the more common doping levels only 30-40 percent of the melt can be crystalized.

### III. Spectroscopy of Nd:YAG

Knowledge of emission and absorption spectra is essential in the study of any laser material. In this section, the spectra for Nd:YAG are discussed with emphasis on those areas relating to the performance of Nd:YAG as a laser material. Also, the fundamental spectroscopic parameters are defined and methods of determining them discussed. Finally, various values of selected spectroscopic parameters for Nd:YAG are presented and the discrepancies among them discussed.

#### Absorption and Emission in Nd:YAG

The optical and near-infrared absorption and emission observed in Nd:YAG are primarily due to transitions between energy states within the 4f subshell. Now, 4f→4f electric dipole transitions are not allowed in the free ion by Laporte's rule since the 4f wavefunctions all have the same parity. However, placing neodymium ions in the crystal field of YAG causes the 4f wavefunctions to have mixed parities leading to the so-called forced electric dipole or Laporte forbidden transitions between the 4f states (Ref 10:118).

The energy level diagram for Nd:YAG can be derived from the absorption and emission spectra. A partial energy level diagram for Nd:YAG is presented in Fig. 3a with the energy level term designators based on the Russell-Saunders coupling scheme. The most intense absorption bands involve transitions from the ground state ( ${}^4I_{9/2}$ ) to the  ${}^4F_{5/2}+{}^2H_{9/2}$  and  ${}^4F_{7/2}+{}^4S_{3/2}$  levels which correspond to wavelength ranges of 7300-7700 ang-

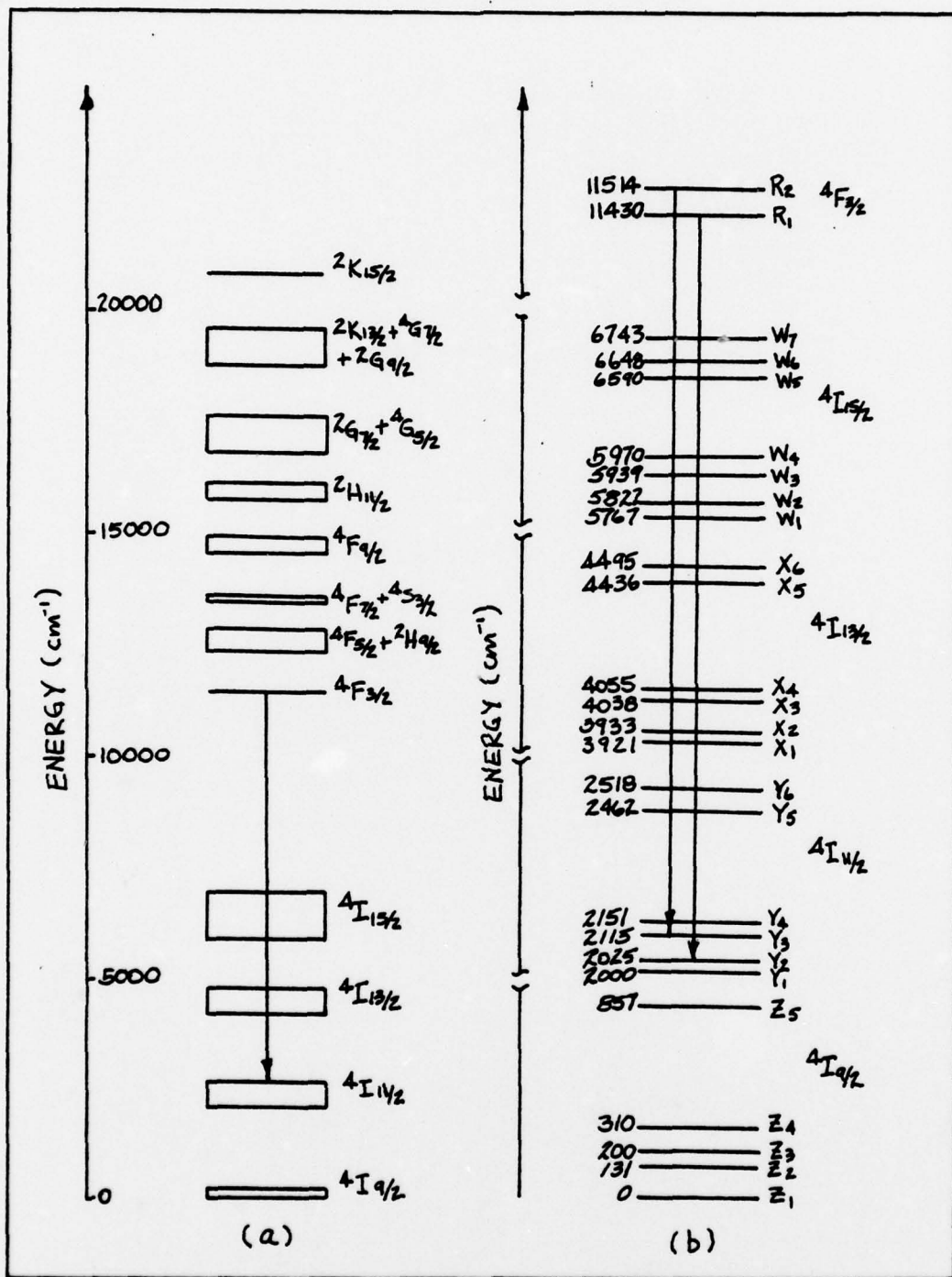


Fig. 3. Energy Levels in Nd:YAG. (a) Partial Energy Level Diagram for Nd in YAG at 4.2 °K (Ref 19:A712). (b) Stark Splittings of the  $4F_{3/2}$  and  $4I$  manifolds at 77 °K (Ref 20:451).

stroms and 7900-8300 angstroms (Ref 17:34-35). According to Brandewie and Telk (Ref 18), all the levels below the  ${}^4D_{3/2}$  (3550 angstroms) relax nonradiatively to the upper laser level ( ${}^4F_{3/2}$ ), therefore, the best pump sources for Nd:YAG are those with large fractions of their spectral output in the 7300-8300 angstrom range.

Since, for the typical excitation wavelengths used with Nd:YAG, all the fluorescent emissions originate from the  ${}^4F_{3/2}$  manifold, the relevant energy levels for the emission spectrum are those shown in Fig. 3b. As indicated in that figure, the  $(2J+1)$ -fold degeneracy of the various manifolds predicted by the Russell-Saunders coupling for the free ion has been partially removed due to the effects of the crystal field. The resulting levels are referred to as Stark levels and, in Fig. 3b, are labeled according to the convention used by Dieke (Ref 10). For Nd:YAG, each of the Stark levels is itself doubly degenerate (Ref 21:2569). Fluorescent emission from the  ${}^4I$  manifolds has not been observed and it is assumed that these levels rapidly relax nonradiatively to the ground state. As indicated by the arrows in Fig. 3b, the laser transition ( $\lambda=1.06\mu$ ) for Nd:YAG is actually a composite of the  $R_2-Y_3$  and  $R_1-Y_2$  transitions between the  ${}^4F_{3/2}$  and  ${}^4I_{11/2}$  manifolds (Ref 22).

#### Fundamental Spectroscopic Parameters

In the study of laser materials, certain spectroscopic parameters are frequently used to describe the merits of a material as a laser medium. The more important of these para-

meters are discussed below.

Lineshape. The dominant line-broadening mechanism in Nd:YAG is thermal broadening (a homogeneous mechanism), therefore, the lineshape for Nd:YAG is Lorentzian (Ref 23:362). The normalized Lorentzian lineshape function can be expressed as:

$$g(\nu) = \frac{\Delta\nu}{2\pi} \{(\nu - \nu_0)^2 + (\Delta\nu/2)^2\}^{-1} \quad (3)$$

where,  $\nu$  = frequency

$\nu_0$  = frequency at line center

$\Delta\nu$  = full width of the line at half maximum,

and the relation

$$\int g(\nu) d\nu = 1 \quad (4)$$

is satisfied. From equation (3), it is clear that the value of a quantity as a function of frequency,  $P(\nu)$ , is related to its value at line center,  $P_0$ , by

$$P(\nu) = \frac{\pi\Delta\nu}{2} P_0 g(\nu) \quad (5)$$

From equations (4) and (5), one obtains the expression

$$\int P(\nu) d\nu = \frac{\pi\Delta\nu}{2} P_0 \quad (6)$$

which relates the area under the Lorentzian line to the line-width and the value of the quantity at line center.

Lifetimes. An atom in an excited state,  $i$ , can spontaneously decay to some lower state,  $j$ , by emitting a photon (radiative decay) or a phonon (nonradiative decay). If the probability of a radiative  $i$ - $j$  transition is given by  $A_{ij}^r$ ,

and that of a nonradiative i-j transition by  $A_{ij}^{nr}$ , then the probability of an i-j transition,  $A_{ij}$ , is given by

$$A_{ij} = A_{ij}^r + A_{ij}^{nr} \quad (7)$$

where all the transition probabilities are expressed in  $\text{sec}^{-1}$ . The lifetime of the i-j transition,  $\tau_{ij}$ , is defined as

$$\tau_{ij} = \frac{1}{A_{ij}} \quad (8)$$

In a similar manner, the radiative and nonradiative terms in equation (7) can be expressed in terms of lifetimes leading to the expression

$$\frac{1}{\tau_{ij}} = \frac{1}{\tau_{sp}} + \frac{1}{\tau_{ij}^{nr}} \quad (9)$$

where,  $\tau_{sp}$  = the spontaneous radiative lifetime of the i-j transition =  $(A_{ij}^r)^{-1}$ ,

$\tau_{ij}^{nr}$  = the nonradiative lifetime of the i-j transition =  $(A_{ij}^{nr})^{-1}$ .

The total transition probability of the  $i^{\text{th}}$  state is determined by summing equation (7) for all j. The lifetime corresponding to this total transition probability will be referred to here as the fluorescent lifetime,  $\tau_f$ , and is related to the transition probability by

$$\frac{1}{\tau_f} = \sum_j A_{ij} \quad (10)$$

Substituting equation (7) into (10) yields

$$\frac{1}{\tau_f} = \sum_j (A_{ij}^r + A_{ij}^{nr}) = \sum_j A_{ij}^r + \sum_j A_{ij}^{nr} \quad (11)$$

which can be written as

$$\frac{1}{\tau_f} = \frac{1}{\tau_r} + \frac{1}{\tau_{nr}} \quad (12)$$

where  $\tau_r$  is the radiative lifetime of the  $i^{\text{th}}$  state and  $\tau_{nr}$  is the nonradiative lifetime of the  $i^{\text{th}}$  state corresponding to  $(\sum_j A_{ij}^r)^{-1}$  and  $(\sum_j A_{ij}^{nr})^{-1}$  respectively.

Of the various lifetimes discussed above, only  $\tau_f$  can be measured directly. The other lifetimes may be calculated from the relationships presented here and in following sections.

Cross Sections. The concept of cross sections is often used in spectroscopy as an alternate means of expressing transition probabilities. Some of the more important relationships involving cross sections are developed below using the approach found in DiBartolo (Ref 24:406-411).

The absorption cross section for a transition is defined by

$$\sigma(\nu) = \frac{k(\nu)}{n_l} \quad (13)$$

where  $k(\nu)$  = absorption coefficient at frequency  $\nu$  ( $\text{cm}^{-1}$ ),  
 $n_l$  = population density of the lower level of the transition ( $\text{cm}^{-3}$ ).

For low intensity excitations, DiBartolo (Ref 24:409) has shown that

$$\int k(\nu) d\nu = \frac{\lambda^2 g_u n_l^e}{8\pi g_l \tau_{sp}} \quad (14)$$

where  $\lambda$  = transition wavelength in the material (cm),  
 $g_u$  = degeneracy of the upper level,  
 $g_l$  = degeneracy of the lower level,  
 $n_l^e$  = population density of the lower level for zero  
excitation intensity ( $\text{cm}^{-3}$ ),  
 $\tau_{sp}$  = spontaneous radiative lifetime of the u-l tran-  
sition (sec).

Thus, equation (13) can be rewritten as

$$\int \sigma(\nu) d\nu = \frac{\lambda^2 g_u}{8\pi g_l \tau_{sp}} \quad (15)$$

since for low excitation intensities  $n_l \approx n_l^e$ . Using the re-  
sult of equation (6) in (15) yields

$$\frac{\pi}{2} \Delta\nu \sigma_0 = \frac{\lambda^2 g_u}{8\pi g_l \tau_{sp}} \quad (16)$$

where  $\sigma_0 = \sigma(\nu_0)$ . Therefore, the peak absorption cross sec-  
tion is given by

$$\sigma_0 = \frac{\lambda^2}{4\pi^2 \Delta\nu} \frac{g_u}{g_l \tau_{sp}} \quad (17)$$

In Nd:YAG, the degeneracies of the various Stark levels are  
the same, therefore, the Einstein B coefficients are equal.  
Also, since Nd:YAG is isotropic,  $\tau_{sp}$  can be replaced by  
 $(A_{ul})^{-1}$  where  $A_{ul}$  is the Einstein A coefficient. Substituting  
 $g_u = g_l$  and  $\tau_{sp} = (A_{ul})^{-1}$  in (17) and recalling that

$$B_{ul} = \frac{\lambda^3}{8\pi h} A_{ul} \quad (18)$$

yields

$$B_{ul} = B_{lu} = \frac{\pi \lambda \Delta \nu}{2h} \sigma_0 \quad (19)$$

Thus, for Nd:YAG, the absorption cross section and the induced emission cross section are equal, and are given by equation (17) with  $g_u/g_l = 1$ .

In those cases where the absorption coefficient can be measured directly, the determination of  $\sigma$  from equation (13) is straight forward. However, direct absorption measurements are not always possible and an alternate method of determining  $\sigma$  is necessary. One such method depends on the relationship between the induced emission cross sections and fluorescent intensities of the lines in the fluorescence spectrum derived below.

The peak emission intensity in watts of the i-j transition,  $I_{ij}$ , can be expressed as

$$I_{ij} = A_{ij}^r h \nu_{ij} N_i \quad (20)$$

where,  $A_{ij}^r$  = radiative transition probability of the i-j transition,

$h \nu_{ij}$  = energy of the emitted photon,

$N_i$  = number of atoms in the initial state.

Then the ratio of the fluorescent intensities of i-j and l-k transitions is given by

$$\frac{I_{ij}}{I_{lk}} = \frac{A_{ij}^r v_{ij} N_i}{A_{lk}^r v_{lk} N_l} \quad (21)$$

Using the results of equation (17) with the ratio of the degeneracies equal to one, allows equation (21) to be rewritten as

$$\frac{I_{ij}}{I_{lk}} = \frac{\Delta v_{ij} \sigma_{ij} v_{ij} \lambda_{lk}^2 N_i}{\Delta v_{lk} \sigma_{lk} v_{lk} \lambda_{ij}^2 N_l} \quad (22)$$

where the  $\sigma$ 's are the peak cross sections. If the initial levels are in thermal equilibrium

$$\frac{N_i}{N_l} = \exp\{-(E_i - E_l)/kT\} = a_{il} \quad (23)$$

Substitution of equation (23) into equation (24) and some rearrangement leads to

$$\frac{\sigma_{lk}}{\sigma_{ij}} = \frac{\Delta v_{ij} v_{ij}^3 n_{ij}^2 I_{lk} a_{il}}{\Delta v_{lk} v_{lk}^3 n_{lk}^2 I_{ij}} \quad (24)$$

where  $n$  is the index of refraction. Therefore, if the emission cross section of one transition is known, the remaining emission cross sections can be determined from the fluorescence data and equation (24).

Branching Ratios. The branching ratio,  $\beta_{ij}$ , is a measure of the fraction of the total fluorescence emitted into the  $i$ - $j$  transition. When specified in terms of photon rates, the branching ratio is given by

$$\beta_{ij} = \frac{I_{ij}/h\nu_{ij}}{\sum_{i,j} (I_{ij}/h\nu_{ij})} \quad (25)$$

where  $I_{ij}$  is the same as in equation (20). If one takes into account the finite width of the emission line and substitutes for the frequency in terms of wavelength, equation (25) becomes

$$\beta_{ij} = \frac{\int \lambda I_{ij}(\lambda) d\lambda}{\sum_{i,j} \int \lambda I_{ij}(\lambda) d\lambda} \quad (26)$$

where the integral in the numerator is over the i-j emission line and the term in the denominator is the sum of all such integrals. Normally, the integrals in equation (26) are determined from the fluorescence spectrum using a planimeter or by the following approximation. Recall that for Nd:YAG the emission lines are fairly sharp and can be characterized by the Lorentzian lineshape function. For sharp lines  $\lambda$  is essentially constant over the line and equation (26) can be approximated by

$$\beta_{ij} = \frac{\lambda_{ij} \int I_{ij}(\lambda) d\lambda}{\sum_{i,j} \lambda_{ij} \int I_{ij}(\lambda) d\lambda} \quad (27)$$

where  $\lambda_{ij}$  is the wavelength corresponding to the peak of the emission line. For a Lorentzian lineshape, the integrals in equation (27) can be evaluated by means of equation (6) in terms of peak emission intensities and linewidths. Singh, et al., have used both of the above methods for determining branching ratios in Nd:YAG and obtained excellent agreement between the two methods (Ref 21).

Another important relationship involving the branching ratios is derived below after the method of Rushworth, et al. (Ref 25:34-35). From equations (20) and (25)

$$\beta_{ij} = \frac{A_{ij}^r N_i}{\sum_{i,j} A_{ij}^r N_i} \quad (28)$$

For a system in thermal equilibrium,  $N_i$ , the population of the  $i^{\text{th}}$  state is related to  $N_g$ , the population of the ground state by

$$N_i = N_g \exp\{-(E_i - E_g)/kT\} = N_g a_{ig} \quad (29)$$

Substituting for  $N_i$  in equation (28) yields

$$\beta_{ij} = \frac{A_{ij}^r a_{ig}}{\sum_{i,j} A_{ij}^r a_{ig}} \quad (30)$$

Since the  ${}^4F_{3/2}$  manifold of Nd:YAG is composed of two Stark levels that are in thermal equilibrium (Ref 22:291), the statistical average of the total radiative transition probability of the manifold is given by

$$\bar{A} = \frac{\sum_{i,j} A_{ij}^r a_{ig}}{\sum_i a_{ig}} \quad (31)$$

From the relationship between lifetimes, the radiative lifetime of the  ${}^4F_{3/2}$  manifold can be expressed as

$$\tau_r = \frac{1}{\bar{A}} = \frac{\sum_i a_{ig}}{\sum_{i,j} A_{ij}^r a_{ig}} \quad (32)$$

Dividing equation (30) by equation (32) yields

$$\frac{\beta_{ij}}{\tau_r} = \frac{A_{ij}^r a_{ig}}{\sum_i a_{ig}} \quad (33)$$

or,

$$A_{ij}^r = \frac{\beta_{ij} \sum_i a_{ig}}{\tau_r a_{ig}} = \frac{1}{\tau_{sp}} \quad (34)$$

Substitution of equation (34) for  $\tau_{sp}$  in equation (17) with  $g_u/g_l = 1$  gives

$$\tau_r = \frac{\beta_{ij} \lambda^2 \sum_i a_{ig}}{\sigma_0 4\pi^2 \Delta\nu a_{ig}} \quad (35)$$

where  $\sigma_0$  is the peak cross section of the i-j transition and  $\Delta\nu$  the corresponding linewidth. Thus, the radiative lifetime of the  ${}^4F_{3/2}$  manifold can be calculated from experimentally determined values of the branching ratios, linewidths, and cross sections.

Quantum Efficiency. The term quantum efficiency is used differently by the spectroscopist and the laser scientist. In spectroscopy, the quantum efficiency,  $\eta_R$ , is usually defined by

$$\eta_R = \frac{\text{number of photons emitted from } i^{\text{th}} \text{ level}}{\text{number of photons absorbed by the material}} \quad (36)$$

and is a measure of the overall fluorescent efficiency of a particular level. As stated previously, in Nd:YAG each pump photon absorbed relaxes nonradiatively to the  ${}^4F_{3/2}$  manifold, therefore,  $\eta_R$  can be expressed as the ratio of the radiative transition probability of the  ${}^4F_{3/2}$  manifold and the total transition probability of the manifold. Therefore, in terms of lifetimes

$$\eta_R = \frac{\tau_f}{\tau_r} \quad (37)$$

When the laser scientist uses the term quantum efficiency, he is most often referring to the fluorescent efficiency of the laser transition. That is:

$$\eta_L = \frac{\text{number of photons emitted in laser transition}}{\text{number of photons absorbed by the material}} \quad (38)$$

For the Nd:YAG  ${}^4F_{3/2}$  manifold, the same argument used in arriving at equation (37) yields

$$\eta_L = \frac{\tau_f}{\tau_{sp}} = \frac{\tau_f}{\tau_{sp}} \eta_R \quad (39)$$

The values of  $\eta_R$  and  $\eta_L$  are normally calculated from experimental data, however, direct measurements of  $\eta_R$  for the  ${}^4F_{3/2}$  manifold of Nd:YAG have been made (Refs 21,26).

#### Spectroscopic Parameters of Nd:YAG

The values of selected spectroscopic parameters of Nd:YAG are presented in Table I. The values of  $\tau_f$  and  $\eta_R$  are for the  ${}^4F_{3/2}$  manifold and those of  $\sigma_0$  and  $\tau_{sp}$  are for the laser transition. The multiple values of  $\sigma_0$ ,  $\tau_{sp}$ , and  $\eta_R$  of Neeland and Evtuhov were determined by different methods using the same sample. Also, Singh, et al., and Kushida, et al., performed their measurements on the same sample.

It is clear from Table I that, with the exception of the fluorescent lifetime, there is little agreement among the various investigators. This disagreement has created a controversy over the role of nonradiative processes in the decay of the  ${}^4F_{3/2}$  manifold and led to speculation that it may be possible to affect significant improvements in the overall efficiency of Nd:YAG as a laser material (Ref 31). This controversy is discussed briefly in the final section of this report.

Table 1  
Spectroscopic Parameters of Nd:YAG

Concentration of Nd (atom %)	$\tau_f$ ( $10^{-6}$ sec)	$\sigma_q$ ( $10^{-19}$ cm <sup>2</sup> )	$\tau_{sp}$ ( $10^{-6}$ sec)	$\eta_R$	Source
1.0	236	3.5 2.7	590 758	1.0 0.8	Neeland and Evtuhov (Ref 27)
1.0	230	8.8	550	1.0	Kushida, et al. (Ref 22)
1.0	230	5.0	X	0.56	Singh, et al. (Ref 21)
1.3	240	8.8	X	X	Birnbaum (Ref 28)
0.85	X	7.0	X	X	Weber (Ref 29)
1.13	X	5.6	890	X	Alves (Ref 30)

#### IV. Power Output from Nd:YAG Lasers

The laser literature is full of expressions for predicting the power output of various laser systems in the different operating modes. However, in the majority of these expressions the fundamental parameters of the host material do not appear explicitly, making it difficult to correctly deduce the functional dependence of power output on the host parameters. In this chapter, the basic expressions for a four level laser system are presented in terms of the fundamental host parameters and the host parameters that are most likely responsible for power output variations in Nd:YAG are identified and discussed.

##### Nd:YAG as a Four Level Laser

The distinguishing feature of four level lasers is the position of the terminal laser level. In four level lasers, this level is far enough above the ground level that its thermal population with respect to that of the ground level is negligible. Recall, from Fig. 3b, that in Nd:YAG the terminal level is approximately  $2000 \text{ cm}^{-1}$  above the ground state, therefore, the thermal population of this level is smaller than that of the ground state by a factor of  $10^{-5}$ . Thus, Nd:YAG can be modeled using a four level scheme such as that illustrated in Fig. 4. In this somewhat simplified model,  $R$  atoms per second are excited from the ground level (1) to the pump level (4). These atoms (in the case of Nd) relax non-radiatively to the upper laser level (3) in a time,  $\tau_4$ , that

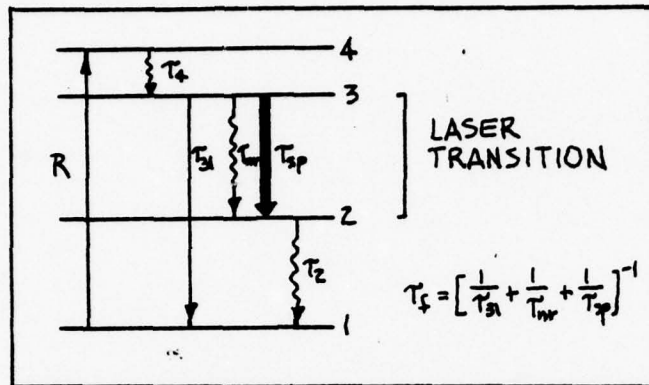


Fig. 4. Schematic of a Four Level Laser Medium

is short compared to the lifetime of the upper laser level,  $\tau_f$ . Relaxation from level 3 may occur by a radiative 3-2 transition (laser transition), a nonradiative 3-2 transition, or radiative and nonradiative 3-1 transitions. Therefore, only a fraction of the atoms in level 3 contribute to the 3-2 radiative transitions. This fraction corresponds to the quantum efficiency,  $\eta_L$ . In the case of Nd, the atoms in level 2 undergo nonradiative transitions to the ground level in a time,  $\tau_2$ , that is short compared to the lifetime of level 3. Since  $\tau_2 \ll \tau_f$ , the population of the lower level is essentially unchanged from its thermal equilibrium value. Thus, the population inversion,  $\Delta N$ , varies as the population of the upper laser level,  $N_3$ .

#### The Gain Coefficient

Recall that induced transitions differ from spontaneous transitions in several important ways. The most obvious difference is that induced transitions occur in both directions while spontaneous transitions are always emission processes.

Also, spontaneous emission is independent of the field intensity while the induced processes are not. This dependence on field intensity is reflected in the induced transition probability rate,  $W_i(\nu)$ , which from Ref 32 and Ref 33:82 is given by

$$W_i(\nu) = \frac{\lambda^2 I_\nu}{8\pi h \nu \tau_{sp}} g(\nu) \quad (40)$$

where,  $I_\nu$  = intensity of the incident field at frequency  $\nu$   
(watts/cm<sup>2</sup>)

$g(\nu)$  = normalized lineshape

$\tau_{sp}$  = radiative lifetime of the transition.

Finally, spontaneous emission produces photons that have no definite phase or directional relationship with the incident field while induced emission produces photons that are coherent with respect to the incident field and are emitted in the same direction as the incident field. Thus, each photon resulting from induced emission contributes to the intensity of the incident field while only a small number of the spontaneous photons do.

Next, in the manner of Ref 33:83, consider the case where a monochromatic plane wave of frequency  $\nu$  and intensity  $I_\nu$  is incident on a medium having  $n_3$  atoms per unit volume in level 3 and  $n_2$  atoms per unit volume in level 2. From the preceding discussion it is clear that the only significant interactions between the medium and the incident field are the result of induced transitions. Therefore, the power per unit volume exchanged by the field and the medium is given by

$$\frac{P}{\text{Volume}} = (n_3 - n_2) W_1(\nu) h\nu \quad (41)$$

where  $W_1(\nu)$  is defined in equation (40). As discussed above, induced transitions are coherent with respect to the incident field, so equation (41) may be interpreted as the change in intensity per unit length ( $dI_\nu/dz$ ). Substituting equation (40) into (41) yields

$$\frac{dI_\nu}{dz} = (n_3 - n_2) \frac{\lambda^2 g(\nu)}{8\pi\tau_{sp}} I_\nu \quad (42)$$

Equation (42) has the solution

$$I_\nu(z) = I_\nu(0) \exp\{\gamma(\nu)z\} \quad (43)$$

where  $I_\nu(0)$  is the initial intensity and  $\gamma(\nu)$  is the gain coefficient defined by

$$\gamma(\nu) = (n_3 - n_2) \frac{\lambda^2 g(\nu)}{8\pi\tau_{sp}} \quad (44)$$

From equations (43) and (44), it is clear that when  $n_3 > n_2$ , the incident wave is amplified and laser action may occur.

#### Gain Saturation in a Homogeneously Broadened Laser Medium

From equation (44) it appears that once a given population inversion is achieved the gain coefficient is fixed. However, that is not the case. When a field is present the inversion tends to decrease from its zero field value because the population of the upper level is greater than that of the lower level but the induced transition probability rate,  $W_1(\nu)$ , is the same. The exact dependence of the populations on field

intensity can only be determined from a rate equation analysis such as the one that follows. The method used here is similar to that of Yariv (Ref 33:90-93).

Consider a four level system such as that depicted in Fig. 4 except that now a monochromatic plane wave of intensity  $I_\nu$  and frequency  $\nu$  corresponding to the 3-2 transition is incident on the medium. Therefore, it is necessary to introduce the induced transition probability,  $W_1(\nu)$ , to account for the interaction of the incident wave and the medium. The resulting rate equations for levels 3 and 2 assuming homogeneous broadening are:

$$\frac{dn_3}{dt} = R_p - \frac{n_3}{\tau_f} - (n_3 - n_2)W_1(\nu) \quad (45)$$

and

$$\frac{dn_2}{dt} = \frac{N_3}{\tau_{sp}} + (n_3 - n_2)W_1(\nu) - \frac{n_2}{\tau_2} \quad (46)$$

Under steady state conditions these equations can be rewritten as:

$$n_3 = \frac{R_p + n_2 W_1(\nu)}{\{(1/\tau_f) + W_1(\nu)\}} \quad (47)$$

and

$$n_2 = \frac{n_3 \{(1/\tau_{sp}) + W_1(\nu)\}}{\{(1/\tau_2) + W_1(\nu)\}} \quad (48)$$

Solving equations (47) and (48) for  $(n_3 - n_2)$  yields:

$$n_3 - n_2 = \frac{R_p \{ \tau_f - (\tau_f / \tau_{sp}) \tau_2 \}}{1 + \{ \tau_f + (1 - (\tau_f / \tau_{sp})) \tau_2 \} W_1(\nu)} \quad (49)$$

Now,  $\tau_f / \tau_{sp}$  is always less than or equal to unity and for this model  $\tau_2$  is short compared to  $\tau_f$ . Therefore, equation (49) can be rewritten as

$$n_3 - n_2 = \frac{R_p \tau_f}{1 + \tau_f W_1(\nu)} = \frac{\Delta n_0}{1 + \tau_f W_1(\nu)} \quad (50)$$

where  $\Delta n_0 = R_p \tau_f$  is the value of the inversion in the absence of a field. Substitution of equation (40) into equation (50) yields

$$n_3 - n_2 = \frac{\Delta n_0}{1 + I_\nu / I_s} \quad (51)$$

where,  $I_s$  is the saturation intensity defined as

$$I_s = \frac{8\pi h\nu \tau_{sp}}{\lambda^2 g(\nu) \tau_f} \quad (52)$$

and corresponds to the value of  $I_\nu$  for which the population inversion has decreased to half its zero field value.

From equations (44) and (51) the gain coefficient can be expressed as

$$\gamma(\nu) = \frac{\Delta n_0 \lambda^2 g(\nu)}{8\pi \tau_{sp} (1 + I_\nu / I_s)} = \frac{\gamma_0(\nu)}{1 + I_\nu / I_s} \quad (53)$$

The decrease in the gain coefficient with  $I_\nu$  predicted by equation (53) is termed gain saturation and (as is discussed in the following section) is responsible for the steady state behavior of laser oscillators.

## Laser Oscillation

Consider a laser resonator such as that shown in Fig. 5 where the laser medium has a gain coefficient,  $\gamma(\nu)$ , and a

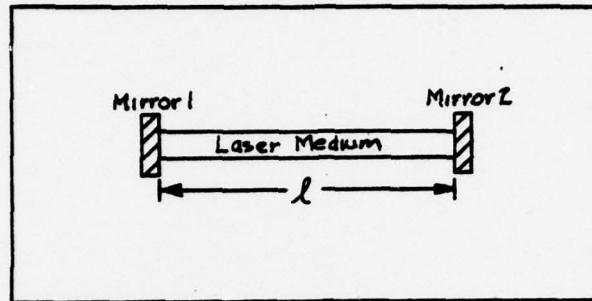


Fig. 5. A Simple Laser Resonator

loss coefficient,  $\alpha$ . An optical field with an initial intensity  $I_0$  will have an intensity  $I$ , after one round trip in the resonator, given by:

$$I = I_0 R_1 R_2 \exp\{2(\gamma(\nu) - \alpha)l\} \quad (54)$$

where  $R_1$  and  $R_2$  are the power reflectivities of the mirrors. For oscillation to occur, the minimum intensity after the round trip must be equal to  $I_0$ . This occurs when:

$$R_1 R_2 \exp\{2(\gamma(\nu) - \alpha)l\} = 1 \quad (55)$$

Substituting  $R_1 = r_1^2$  and  $R_2 = r_2^2$  into equation (55) and solving for  $\gamma(\nu)$  yields:

$$\gamma_t(\nu) = \alpha - \frac{1}{2l} \ln(r_1 r_2) \quad (56)$$

where the subscript 't' indicates that this is the minimum or threshold value of the gain coefficient for oscillation to occur. Similarly, from equations (44) and (56), the threshold value for the population inversion is defined by:

$$n_t = (n_3 - n_2)_t = \frac{8\pi\tau_{sp}}{\lambda^2 g(\nu)} \left\{ \alpha - \frac{1}{L} \ln(r_1 r_2) \right\} \quad (57)$$

For the case where the frequency of the incident field corresponds to the center frequency,  $\nu_0$ , of the 3-2 transition, substitution for  $g(\nu_0)$  from equation (3) yields

$$n_t = \frac{4\pi^2 \Delta\nu\tau_{sp}}{\lambda^2} \left\{ \alpha - \frac{1}{L} \ln(r_1 r_2) \right\} \quad (58)$$

Recall from equation (51) that the population inversion decreases as the radiation intensity increases due to the increase in induced transitions. However, when the inversion falls below the threshold value of equation (58), laser oscillation ceases, the radiation intensity is essentially zero, and the population inversion begins to increase again. When the inversion reaches threshold, oscillation starts again and the inversion begins to decrease. Due to this saturation behavior, the value of the steady state population inversion is the same as the threshold value. Therefore, at steady state each atom in the upper laser level in excess of the threshold population results in a laser transition in order to restore the population inversion to the threshold value.

#### Power Output for CW Operation

From the preceding discussion, it is clear that for CW operation the population inversion density must be maintained at the threshold value given by equation (58). Thus, the population density of the upper laser level must be maintained at

$$n_3 = n_2 + n_t \quad (59)$$

For an ideal four level system the thermal population of the lower laser level,  $n_2$ , is essentially zero and can be neglected with respect to  $n_t$ . This assumption is not a good one for Nd:YAG, since for one atom percent doping the thermal population of the lower laser level is roughly  $10^{15}$  atoms/cm<sup>3</sup> which is of the same order as the value for  $n_t$  given by Yariv (Ref 33:149). However, the main point of this section is to determine the variation of power output as a function of the host parameters. Neglecting  $n_2$  with respect to  $n_t$  does not change the functional dependence of the power output on the host parameters and does result in a somewhat simpler expression for power output, therefore, the assumption that  $n_2 \approx 0$  will be made.

Under the further assumption that each pump photon absorbed excites an ion into the upper laser level, the minimum photon pumping rate is

$$R_{\min} = \frac{n_t V}{\eta_L \tau_f} \quad (60)$$

where the quantum efficiency,  $\eta_L$ , accounts for the fact that only a fraction of the excited ions produce radiation at the laser frequency and  $V$  is the volume of the material. For pumping rates ( $R$ ) greater than  $R_{\min}$ , laser oscillation occurs and each excited ion produces a laser photon of frequency  $\nu$ . Thus, the power output for CW operation is given by

$$P_o = h\nu(R - R_{\min}) \quad (61)$$

This equation can be rewritten in terms of host parameters by means of equations (60), (58), and (39) yielding

$$P_o = hv(R - \frac{4\pi^2 V v^2 \Delta v n^2 \tau_{sp}^2 \{\alpha - (1/l) \ln(r_1 r_2)\}}{c^2 \tau_f^2}) \quad (62)$$

where  $n$  is the index of refraction and the relation  $\lambda = c/nv$  has been used.

### Energy Output for Q-Switch Operation

In contrast to the relatively simple development that led to equation (62), the development of a similar relationship for Q-switch operation is rather complex. The approach used here is after that of Wagner and Lengyel (Ref 34:2040-42) and assumes, in addition to the assumptions of the previous section, that:

- 1). Replenishment of the inversion by the pump during the life of the pulse is negligible.
- 2). No change in the inversion occurs during the switching process - i.e. fast switching.
- 3). The effects of continuous pumping and spontaneous emission on the inversion are neglected.

From Fig. 5, the optical path length in the oscillator is  $n\ell$  where  $n$  is the index of refraction of the material and the time of transit is

$$t^1 = n\ell/c \quad (63)$$

Recall that the cavity lifetime is defined as

$$t_c = n\ell/cL \quad (64)$$

where  $L$  is the total single pass loss given by

$$L = \alpha l - \ln(r_1 r_2). \quad (65)$$

If  $\gamma l$  is the gain per pass and  $\phi$  is the number of photons, then the rate of increase in photons is  $\phi \gamma l / t^1$  and the rate of decrease is  $\phi / t_c$ . Thus

$$\frac{d\phi}{dt} = \{(\gamma l / t^1) - (1 / t_c)\} \phi \quad (66)$$

For each photon produced the total inversion population,  $N$ , is decreased by 2, therefore

$$\frac{dN}{dt} = -2(\gamma l / t^1) \phi \quad (67)$$

Let  $\tau = t / t_c$ , then equations (66) and (67) become

$$\frac{d\phi}{d\tau} = \{(\gamma / \gamma_t) - 1\} \phi \quad (68)$$

and

$$\frac{dN}{d\tau} = -2 \frac{\gamma}{\gamma_t} \phi \quad (69)$$

where  $\gamma_t = t^1 / l t_c$  is the threshold gain. Since  $\gamma \propto N$ ,  $\gamma / \gamma_t$  can be replaced by  $N / N_t$  with the results

$$\frac{d\phi}{d\tau} = \{(N / N_t) - 1\} \phi \quad (70)$$

and

$$\frac{dN}{d\tau} = -2(N / N_t) \phi \quad (71)$$

Dividing equation (70) by (71) and integrating yields

$$\phi = \frac{1}{2} \{N_t \ln(N / N_t) - (N - N_t)\} \quad (72)$$

since the initial number of photons,  $\phi_i$ , is zero if spontaneous emission is neglected. Also, substitution of equation (70) into (71) and some rearranging results in

$$\frac{d(N+2\phi)}{dt} = -2\phi \quad (73)$$

The number of photons emitted in a single pulse is obtained from (73) by integrating over the duration of the pulse and is given by

$$\phi_T = \int \phi dt = \frac{1}{2} \{N_i - N_f + 2(\phi_i - \phi_f)\} \quad (74)$$

of since  $\phi_f \approx \phi_i \approx 0$

$$\phi_T \approx \frac{N_i - N_f}{2} \quad (75)$$

An expression for  $(N_i - N_f)$  in terms of the threshold inversion  $N_t$  is obtained from equation (72) by letting  $\phi = \phi_f \approx 0$  and  $N = N_f$  with the result

$$N_i - N_f = N_t \ln(N_i / N_f) \quad (76)$$

Now, in general the energy stored in the pulse is

$$E_o = \frac{N_i - N_f}{2} h\nu \quad (77)$$

where  $\nu$  is the laser transition frequency. However, two cases are of primary interest.

Case I. For values of  $N_i / N_t > 4$ , Wagner and Lengyel (Ref 34:2042) have shown that  $N_i \gg N_f$ . Therefore, equation (77) reduces to

$$E_o = N_i h\nu / 2 \quad (78)$$

Case II. For  $N_i/N_t \approx 1$ ,  $N_f/N_i \approx 1$  (Ref 34:2042) and equation (76) can be written as

$$\frac{N_i}{N_t} = \frac{\ln(N_f/N_i)}{(N_f/N_i)-1} = \frac{\ln(x)}{x-1} \quad (79)$$

But

$$\ln(x) \approx x-1 - \frac{1}{2}(x-1)^2 + \dots \quad \text{for } 2 \geq x > 0 \quad (80)$$

Therefore

$$\frac{N_i}{N_t} = 1 + \frac{N_i - N_f}{2N_i} \quad (81)$$

or

$$\frac{N_i}{N_t}(N_i - N_t) = \frac{1}{2}(N_i - N_f) \quad (82)$$

Substituting equation (82) into (77) yields

$$E_o = \{(N_i^2/N_t) - N_i\}h\nu \quad (83)$$

Since  $N_t = n_t V / \eta_L$ , where  $n_t$  is given by equation (58)

$$E_o = \left\{ \frac{N_i^2 \lambda^2 \tau_f}{4\pi^2 \Delta v \tau_{sp}^2 (\alpha - (1/l) \ln(r_1 r_2))} - N_i \right\} h\nu \quad (84)$$

or in terms of the laser transition frequency

$$E_o = \left\{ \frac{N_i^2 c^2 \tau_f}{4\pi^2 v^2 n^2 \Delta v \tau_{sp}^2 (\alpha - (1/l) \ln(r_1 r_2))} - N_i \right\} h\nu \quad (85)$$

At first glance, it might seem from equation (78) that the energy in the pulse is independent of the host parameters, however, the validity of the assumption  $N_i/N_t > 4$  depends on the host parameters through  $N_t$ . Thus, the energy output is indirectly dependent on the same host parameters that ap-

pear explicitly in equation (85).

#### Key Host Parameters

The host parameters that may affect the performance of Nd:YAG laser systems are, from inspection of equations (62) and (85), the index of refraction ( $n$ ), the loss coefficient for the laser transition ( $\alpha$ ), the linewidth ( $\Delta\nu$ ), the radiative lifetime of the laser transition ( $\tau_{sp}$ ), and the lifetime of the  ${}^4F_{3/2}$  level ( $\tau_f$ ). While the functional dependence of the equations on these parameters is slightly different, it is clear that in both cases increases in  $n$ ,  $\Delta\nu$ ,  $\alpha$ , and  $\tau_{sp}$  and decreases in  $\tau_f$  result in degradation of laser performance.

The variations of most of the host parameters with temperature and concentration are known. However, the variations in power output, of interest here, are observed between rods with nominally the same concentration and operated under the same thermal conditions. Therefore, the parameters that are more sensitive to variations in concentration and temperature are the ones of primary interest.

In the case of Nd:YAG, the index of refraction is weakly dependent on concentration for normal ( $\approx$ one atom percent) doping levels (Ref 12:91-92) and is essentially constant for small changes in temperature (Ref 8). The linewidth is also a function of temperature since Nd:YAG is thermally broadened. However, for small changes in temperature variations in linewidth are insignificant. There is no evidence to indicate that the linewidth is concentration dependent for the normal concentrations used in Nd:YAG. The radiative lifetime

of the laser transition is independent of temperature (Ref 35: 1100) and, since  $\tau_{sp}$  is determined by the interaction of the fields of the ion and the crystal, the dependence on concentration should be negligible except at extremely high doping levels. The loss coefficient varies directly with the absorption coefficient,  $k(\nu)$ , which is strongly dependent on the population of the terminal laser level (recall equation (14)). The terminal level population is directly proportional to the concentration of neodymium ions and dependent on temperature through the Boltzmann factor ( $\exp\{-\Delta E/kT\}$ ). Also, the loss coefficient exhibits strong dependence on the concentration of impurity ions that can absorb laser radiation and the amount of scattering in the crystal. The lifetime of the upper laser level is essentially independent of temperature (Ref 36:498), but exhibits a rapid decrease with concentration for doping levels above one atom percent (Ref 9 and Ref 13:53).

Based on the preceding discussion, the key host parameters for Nd:YAG appear to be  $\alpha$  and  $\tau_f$ . Indeed, the discussion of energy transfer mechanisms in the next chapter emphasizes mechanisms that would affect these parameters. However, experimental correlations between the variations of the host parameters and laser performance have not been made; therefore, the possibility that another parameter(s) is responsible for the variations in laser performance from rod to rod cannot be neglected.

## V. Energy Transfer Mechanisms

In the previous chapter, variations in laser performance were related to variations in the parameters of the host material. Before the variations in these parameters can be controlled, the mechanism(s) that causes them must be understood. The discussion that follows presents qualitative descriptions of the more common energy transfer mechanisms and their effects on the host parameters, as well as comments on the likelihood that a given mechanism is responsible for variations in these parameters from one rod to the next.

### Resonant Transfer

Consider the case where the metastable  ${}^4F_{3/2}$  level of the neodymium ion coincides with an energy level (above the ground state) of an impurity. These levels are said to be in resonance and energy transfer between the ions may occur. Thus, a neodymium ion in the  ${}^4F_{3/2}$  level may transfer its energy to the impurity ion producing a neodymium ion in the ground state and an excited impurity ion. As illustrated in Fig. 6a, the excited impurity ion may then decay either radiatively or non-radiatively to its ground state.

The net effect of resonant transfer is to deplete the population of the metastable level with no contribution to the fluorescent yield of the laser transition. Since this mechanism represents an additional decay process, it should result in a decrease in the fluorescent lifetime of the  ${}^4F_{3/2}$  level. Furthermore, if the impurity ion decays by radiative

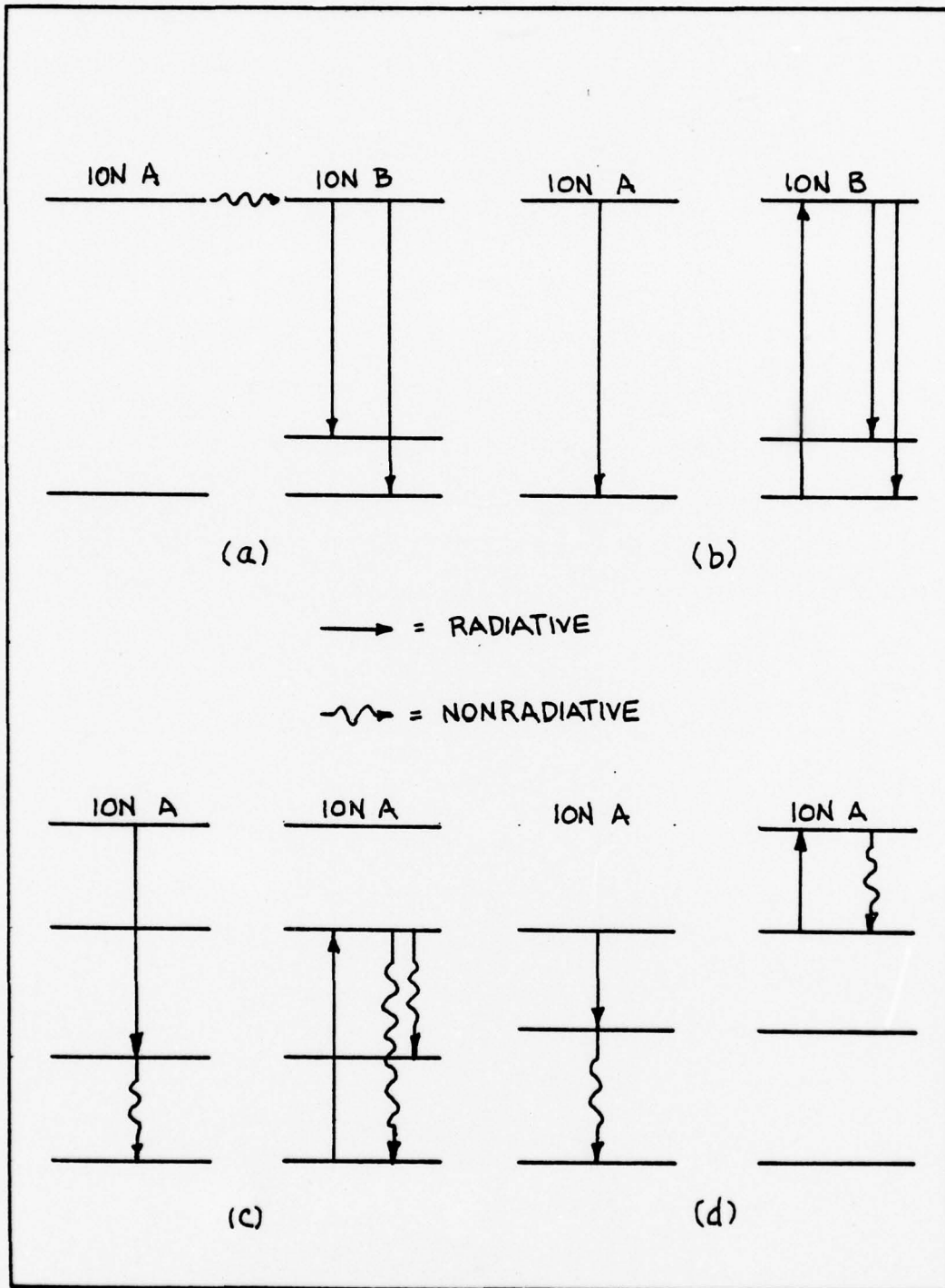


Fig. 6. Energy Transfer Mechanisms: (a) Resonant Transfer, (b) Radiation Trapping, (c) Cross Relaxation, (d) Auger Recombination.

means, it may be possible to identify it from the fluorescence spectrum of the material. The strength of the resonant transfer process depends on the impurity concentration. It is highly unlikely that the impurity concentration is the same for all rods, which could account for rod to rod variations.

#### Radiation Trapping

The term radiation trapping, as used here, refers to the process (see Fig. 6b) whereby an emitted photon encounters an impurity ion with a matching transition or a lattice defect and is reabsorbed.

Since radiation trapping does not involve an interaction with the metastable level of the neodymium ion, it does not affect the fluorescent lifetime. However, this mechanism will increase the loss coefficient of the material. This mechanism, like resonant transfer, is a likely one for explaining the performance variations among rods since it too depends on the concentration of impurity ions or defects. Belt, et al., (Ref 37) have found that substantial amounts of iron are present in the insulating materials used in the growth process. Since iron exhibits significant absorption at  $1.06\mu$ , it should be a prime suspect as the cause of radiation trapping if absorption data indicate the possibility that this mechanism is active in Nd:YAG (Ref 37).

#### Cross Relaxation

Cross relaxation is a process somewhat similar to radiation trapping by an impurity in that it requires matching

transitions. However, in the case of radiation trapping, the emitted photon is reabsorbed, while for cross relaxation, the interaction of ions with such matching transitions results in an entirely different relaxation process. As an example of cross relaxation, consider the case (see Fig. 6c) where an excited neodymium ion interacts with another neodymium ion in the ground state. The excited ion may undergo a radiative transition to one of the  ${}^4I$  manifolds above the  ${}^4I_{11/2}$  state followed by a nonradiative transition to the ground state, while the unexcited ion undergoes a corresponding absorption from the ground state and subsequent nonradiative relaxation back to the ground state. The net result, is depletion of the excited state population with no contribution to the fluorescence at the laser frequency. The probability that cross relaxation will occur depends on the proximity of the interacting ions (concentration) as well as the energy match between the transitions. In those cases where the transitions do not exactly match, cross relaxation, with the absorption or emission of a phonon for energy conservation, may still occur (Ref 24:497).

Since cross relaxation is an alternate decay mechanism for the metastable state, it decreases the fluorescent lifetime. In fact, Danielmeyer has proposed that phonon-assisted cross relaxation involving the  ${}^4F_{3/2}$ - ${}^4I_{15/2}$  and  ${}^4I_{9/2}$ - ${}^4I_{15/2}$  transitions is responsible for the decrease in the fluorescent lifetime of the  ${}^4F_{3/2}$  manifold with neodymium concentration that is observed in Nd:YAG (Ref 38). Singh (Ref 39) has shown

that the mechanism for cross relaxation proposed by Danielmeyer involves the absorption of a phonon from the lattice and would result in the fluorescent lifetime exhibiting strong temperature dependence. Since the fluorescent lifetime is observed to be essentially independent of temperature variations (Ref 36:498), Singh has proposed an alternate mechanism for cross relaxation involving the  ${}^4F_{3/2} - {}^4I_{13/2}$  and  ${}^4I_{9/2} - {}^4I_{15/2}$  transitions and the emission of a phonon. This mechanism predicts a decrease in fluorescent lifetime with neodymium concentration, but essentially no change in lifetime with temperature.

Recall that concentration gradients of 20-30 percent for 20 cm long boules are known to exist in quality boules of Nd:YAG. In the growth of Nd:YAG at concentrations near one atom percent, these gradients may produce Nd concentrations high enough to decrease the fluorescent lifetime of the metastable level thru cross relaxation. Therefore, cross relaxation is another likely cause of performance variations in Nd:YAG rods.

#### Multiphonon Nonradiative Decay

In addition to radiative decay involving photons, excited ions may relax to the ground state by the nonradiative emission of phonons. When the energy gap for a transition exceeds that of the highest energy phonons in the material, nonradiative decay may still occur by the emission of more than one phonon. The transition probability for these multiphonon emission processes is given by

$$W_{mp} = W_0 \left[ \frac{\exp(\hbar\omega_1/kT)}{\exp(\hbar\omega_1/kT)-1} \right]^{p_1} \quad (86)$$

where  $W_0$  is the transition probability for  $T=0$ ,  $\hbar\omega_1$  is the phonon energy, and  $p_1$  is the order of the process determined by

$$p_1 = \frac{\Delta E \text{ of the transition}}{\hbar\omega_1} \quad (87)$$

It has been shown that multiphonon decay generally involves phonons that result in the lowest order process consistent with the cut-off frequency of the phonon spectrum (Ref 40:35-55).

If multiphonon decay is significant in a material, the fluorescent lifetime should decrease with increasing temperature. Recall that the fluorescent lifetime of the metastable level in Nd:YAG is essentially constant with temperature (Ref 36:498). Therefore, multiphonon relaxation is probably not an important decay mechanism in Nd:YAG.

#### Excited State Pumping

If a material is pumped hard enough, the population of the excited state will eventually reach the point where, if a suitable transition exists, the pumping radiation is nearly as likely to be absorbed by an ion in the excited state as by an ion in the ground state. This excited state absorption depletes the population of the metastable level and makes it more difficult to achieve or maintain a population inversion. If

(as in Nd:YAG) the levels above the metastable level relax nonradiatively back to the metastable level, excited state pumping does not deplete the inversion. However, the efficiency of the pump in populating the metastable level is decreased. Continued increases in pump power result in further decreases in pump efficiency and saturation of the fluorescence from the metastable level.

Since the energy of the metastable level of Nd is much greater than that of the ground level, the population of the metastable level is much less than that of the ground level even during laser operation. Therefore, excited state pumping is probably not significant in Nd:YAG.

#### Auger Recombination

If two ions in the metastable level interact, it is possible that one ion will lose its excitation energy to the other producing an ion in a still higher state and an ion in the ground state. If the doubly excited ion relaxes nonradiatively to the metastable level, the net effect of this process is to remove one ion from the excited state population with no contribution to the fluorescent output. This process, illustrated in Fig. 6d, is called Auger recombination (Ref 38).

Auger recombination, is an effective fluorescence quenching process only for pump powers beyond those normally used in laser operation (Ref 38). Therefore, Auger recombination probably does not play a significant role in laser performance under normal operating conditions.

## VI. Recommendations for Future Investigations

From the preceding discussion, it should be clear that, although quite a bit is known about the chemistry, growth, and spectroscopy of Nd:YAG, there are still many questions that need to be answered. Some future investigations that may shed light on the mechanism or mechanisms responsible for the output power variations in Nd:YAG are discussed in the following pages.

At the conclusion of Chapter III, it was mentioned that the discrepancies in the values of the spectroscopic parameters of Nd:YAG had led to speculation that significant improvements in the laser performance of Nd:YAG might be possible. Recent experiments by Singh, et al. (Ref 39), in which single phase powders of Nd:YAG were produced which had significantly longer fluorescent lifetimes than commercial Nd:YAG of the same concentration, seem to support Singh's original assertion that the correct value for the radiative quantum efficiency,  $\eta_R$ , in commercial Nd:YAG is 0.56 (Ref 21) rather than 1.0 (Refs 22,26). If Singh's value for  $\eta_R$  in commercial Nd:YAG is correct, then it may be possible to improve the efficiency of Nd:YAG by a factor of two. Now, the correct value of  $\eta_R$ , whether it is 0.56 or 1.0, has no bearing on rod to rod performance variations if it is constant. However, the value of  $\eta_R$  does provide important information on the role of nonradiative processes in the decay of the  ${}^4F_{3/2}$  level which

may help in determining the mechanism or mechanisms responsible for performance variations in Nd:YAG. Therefore, one goal of future investigations should be to resolve the controversy over the value of  $\eta_R$  in commercial Nd:YAG.

If the mechanism(s) responsible for output variations in Nd:YAG is ever to be determined, then experimental data relating laser performance and variations in the host parameters are essential. Therefore, one of the immediate goals of any further investigations in this area should be to provide that data. One possible approach for doing this is outlined below.

Any investigation into the relationship between host parameters and laser performance must use rods for which the complete growth history, including the position of the rod in the boule, is known. The rods employed should have concentrations of approximately 0.8-1.0 atom percent (the normal range for Nd:YAG). All rods should have the same dimensions and external finish. The CW laser output of each rod should be determined using a standard laser cavity and identical pumping conditions. Once the laser performance of the rods has been determined, the following passive measurements should be made:

- 1). Determine the relative optical quality of the rods using Twyman-Green interferometry.
- 2). Measure the passive absorption from 0.3-2.0 microns at room temperature and at approximately the same temperature as that experienced by the rod during

laser operation.

- 3). Measure  $\tau_f$  as a function of distance along the rod.
- 4). Obtain the fluorescence spectrum of the  ${}^4F_{3/2}$  manifold and determine the branching ratios and laser transition cross section.
- 5). Measure  $\eta_R$  directly (Refs 21,26).
- 6). Determine crystal defect concentration.
- 7). Determine the actual neodymium concentration as a function of distance along the rod.
- 8). Analyze the rods for impurities such as iron that absorb the laser or pump wavelengths.

Clearly, an investigation of the scope of the one just outlined is expensive and time consuming and may never be practical from an economic standpoint. However, unless the number of possible mechanisms can be narrowed down substantially, the above approach may be necessary.

Based on the available data, one possible explanation for the rod to rod variations seems to deserve special consideration. Recall that the low distribution coefficient of neodymium leads to melt enrichment and produces concentration gradients in the boule. Since the fluorescent lifetime is known to decrease rapidly for concentrations above 1.2 atom percent, concentration gradients can result in decreased laser performance. Furthermore, the reported values of the distribution coefficient range from 0.12-0.21, thus, the same starting melt composition and growth conditions may not always produce the same concentration profile in the boule. The net

result is that it is possible that a boule grown to contain a specific neodymium concentration may, in fact, contain a significantly higher concentration than desired and have a correspondingly lower fluorescent lifetime with decreased laser performance.

Experimental confirmation of the preceding hypothesis would involve the following:

- 1). Boules should be grown from the same melt composition and under the same growth conditions.
- 2). Rods should come from the top, middle, and bottom of the boules.
- 3). All rods should have the same dimensions and external finish.
- 4). Evaluate laser performance based on CW power output in a standard cavity.
- 5). Compare optical quality of rods using Twyman-Green interferometry.
- 6). Measure  $\tau_f$  as a function of distance along the rod.
- 7). Determine neodymium concentration as a function of distance along the rod.

If the hypothesis is correct, the rods which exhibit the poorer performance will have shorter fluorescent lifetimes and higher concentrations.

### Bibliography

1. Schawlow, A. L. and Townes, C. H. "Infrared and Optical Masers." Physical Review, 112, 1940-1949, 15 December 1958.
2. Maiman, T. H. "Stimulated Optical Radiation in Ruby Masers." Nature, 187, 493-494, August 1960.
3. Johnson, L. F. and Nassau, K. "Infrared Fluorescence and Stimulated Emission of  $\text{Nd}^{+3}$  in  $\text{CaWO}_4$ ." Proceedings of the IRE, 49, 1704-1706, November 1961.
4. Snitzer, E. "Optical Maser Action of  $\text{Nd}^{+3}$  in a Barium Crown Glass." Physical Review Letters, 7, 444-446, 15 December 1961.
5. Guesic, J. E., et al. "Laser Oscillations in Nd-doped Yttrium Aluminum, Yttrium Gallium, and Gadolinium Garnets." Applied Physics Letters, 4, 182-184, 15 May 1964.
6. Belt, R. F. "YAG: A Versatile Host." Laser Focus, 6, 44-47, April 1970.
7. Osterink, L. M. and Foster, J. D. "Thermal Effects and Transverse Mode Control in a Nd:YAG Laser." Applied Physics Letters, 12, 128-131, 15 February 1968.
8. Osterink, L. M. and Foster, J. D. "Thermal Effects in a Nd:YAG Laser." Journal of Applied Physics, 41, 3656-3663, August 1970.
9. Monchamp, R. R. "Preparation and Properties of Crystalline Laser Oxide Materials." Journal of Solid State Chemistry, 12, 201-206, 1975.
10. Dieke, G. H. Spectra and Energy Levels of Rare Earth Ions in Crystals, edited by H. M. and Hannah Crosswhite. New York, Interscience Publishers, 1968.
11. Smith, W. V. and Sorokin, P. P. The Laser. New York, McGraw-Hill, 1966.
12. Findlay, D. and Goodwin, D. W. "The Neodymium in YAG Laser" in Advances in Quantum Electronics, edited by D. W. Goodwin. London, Academic Press, 77-125, 1970.
13. Belt, R. F. "Nd Concentration in YAG." Laser Focus, 9, 51-53, August 1973.
14. Belt, R. F., et al. "Crystal Growth and Perfection of Large Nd:YAG Single Crystals." Journal of Crystal Growth, 268-271, 1972.

15. Cockayne, B. "Non-Uniform Impurity Distribution in Yttrium Aluminum Garnet Single Crystals." Philosophical Magazine, 12, 943-950, November 1965.
16. Nassau, K. "The Chemistry of Laser Crystals" in Applied Solid State Science, edited by Raymond Wolfe. New York, Academic Press, 174-288, 1971.
17. Kaminskii, A. A. "Stimulated Radiation from YAG:Nd Crystals." Soviet Physics-JETP, 24, 33-39, January 1967.
18. Brandewie, R. A. and Telk, C. L. "Quantum Efficiency of  $Nd^{+3}$  in Glass, Calcium Tungstate, and Yttrium Aluminum Garnet." Journal of the Optical Society of America, 57, 1221-1225, 1967.
19. Konigstein, J. A. and Guesic J. E. "Energy Levels and Crystal Field Calculations of Neodymium in Yttrium Aluminum Garnet." Physical Review, 136, A712-A716, November 1964.
20. Feofilov, P. P., et al. "On the Luminescence of Neodymium and Chromium in Yttrium Aluminum Garnet." Optics and Spectroscopy, 19, 451-452, 1965.
21. Singh, S., et al. "Stimulated Emission Cross Section and Fluorescent Quantum Efficiency for  $Nd^{+3}$  in Yttrium Aluminum Garnet at Room Temperature." Physical Review B, 2566-2572, 15 September 1974.
22. Kushida, T., et al. "Laser Transition Cross Section and Fluorescence Branching Ratios for Nd in Yttrium Aluminum Garnet." Physical Review, 167, 289-291, 10 March 1968.
23. Siegman, A. E. An Introduction to Lasers and Masers. New York, McGraw-Hill, 1971.
24. DiBartolo, B. Optical Interactions in Solids. New York, Wiley and Sons, 1968.
25. Rushworth, P. M., et al. "Final Report: Improved Neodymium Laser Materials." Martin Marietta Corporation, OR 11,942, December 1970.
26. Dianov, E. M., et al. "Direct Measurements of Fluorescent Quantum Yield from the Metastable  ${}^4F_{3/2}$  State of  $Nd^{+3}$  in  $Y_3Al_5O_{12}$  Crystals." Soviet Physics-Doklady, 20, 622-624, September 1975.
27. Neeland, J. K. and Evtuhov, V. "Measurement of the Laser Transition Cross Section for Nd in Yttrium Aluminum Garnet." Physical Review, 156, 244-246, 10 April 1967.

28. Birnbaum, M. and Gelbwachs, J. A. "Stimulated Emission Cross Section of  $\text{Nd}^{+3}$  at 1.06 $\mu$  in  $\text{POCl}_3$ , YAG,  $\text{CaWO}_4$ , ED-2 Glass, and LG55 Glass." Journal of Applied Physics, 43, 2335-2338, May 1972.
29. Weber, M. J. and Varitimos, T. E. "Optical Spectra and Intensities of  $\text{Nd}^{+3}$  in  $\text{YAlO}_3$ ." Journal of Applied Physics, 42, 4996-5005, November 1971.
30. Alves, R. V., et al. "Neodymium-Activated Lanthanum Oxysulfide: A New High-Gain Laser Material." Journal of Applied Physics, 42, 3043-3048, July 1971.
31. Nd:YAG Specification Conference, sponsored by the Space and Missile Systems Organization, 24 August 1976.
32. Yariv, A. and Gordon, J. P. "The Laser." Proceedings of the IEEE, 51, 4-29, January 1963.
33. Yariv, A. Introduction to Optical Electronics. New York, Holt, Rinehart, and Winston Inc., 1971.
34. Wagner, W. G. and Lengyel, B. A. "Evolution of the Giant Pulse in a Laser." Journal of Applied Physics, 34, 2040-2046, July 1963.
35. Thorton, J. R., et al. "Properties of Neodymium Laser Materials." Applied Optics, 8, 1087-1102, June 1969.
36. Zverev, G. M., et al. "Non-radiative Transitions Between Levels of Trivalent Rare-Earth Ions in Yttrium Aluminum Garnet Crystals." Soviet Physics-JETP, 33, 497-501, September 1971.
37. Belt, R. F., et al. "EPR and Optical Study of Fe in Nd:YAlO<sub>3</sub> Laser Crystals." Applied Physics Letters, 25, 218-220, 15 August 1974.
38. Danielmeyer, H. G., et al. "Fluorescence Quenching in Nd:YAG." Applied Physics, 1, 269-274, 1973.
39. Singh, S., et al. Bell Telephone Laboratories, unpublished.
40. Riseberg, L. A. and Weber, M. J. "Relaxation Phenomena in Rare Earth Luminescence." GTE Laboratories Inc., TR74-051.2, July 1974.

## Appendix A

### Supplementary Bibliography

#### Chemistry and Crystal Growth

Geller, S. "Crystal Chemistry of the Garnets." Zeitschrift fur Kristallographie, 125, 1-47, January 1967.

#### Spectroscopic and Laser Parameters

Edwards, J. G. "Measurement of the Cross Section for Stimulated Emission in Neodymium-Doped Glass from the Output of a Free-Running Laser Oscillator." Journal of Physics D, 1, 449-456, 1968.

Guha, J. K. "Spectroscopy and Laser Properties of Neodymium in Yttrium Aluminum Garnet and Yttrium Orthoaluminate." Scientific Report No. 15, Electronic Sciences Laboratory, University of Southern California, June 1973.

Hsu, T. "A Nd:YAG Laser Bibliography." Applied Optics, 11, 1287-1301, May 1972.

Johnson, L. F. "Optical Maser Characteristics of Rare-Earth Ions in Crystals." Journal of Applied Physics, 34, 897-909, April 1963.

Kiss, Z. J. and Pressley, R. J. "Crystalline Solid Lasers." Applied Optics, 5, 1474-1486, October 1966.

Krupke, W. F. "Radiative Transition Probabilities Within the  $4f^3$  Ground Configuration of Nd:YAG." IEEE Journal of Quantum Electronics, 7, 153-159, April 1971.

Nishimura, T. and Omi, T. "Relation Between Laser Characteristics and Nd Ion Concentration in Nd:YAG Crystals." Japan Journal of Applied Physics, 14, 1011-1016, July 1975.

#### Laser Physics

Koechner, W. "Analytical Model of a CW YAG Laser." Laser Focus, April 1970.

Lieberman, I. "High-Power Nd:YAG Continuous Laser." IEEE Journal of Quantum Electronics, 5, 345, June 1969.

Maitland, A. and Dunn, M. H. Laser Physics. London, North-Holland Publishing Co., 1969.

McClung, F. J. and Hellwarth, R. W. "Characteristics of Giant Optical Pulsations from Ruby." Proceedings of the IEEE, 51, 46-53, January 1963.

Weichel, H. and Pedrotti, L. S. "A Summary of Useful Laser Equations - an LIA Report." Electro-Optical Systems Design, 22-36, July 1976.

Yariv, A. Quantum Electronics (Second Edition). New York, John Wiley and Sons, Inc., 1975.

### Energy Transfer

Dexter, D. L. "A Theory of Sensitized Luminescence in Solids." Journal of Chemical Physics, 21, 836-850, May 1953.

Hurrell, J. P., et al. "Optical Phonons of Yttrium Aluminum Garnet." Physical Review, 173, 851-856, September 1968.

Layne, C. B., et al. "Nonradiative Relaxation of Rare-Earth Ions in Silicate Laser Glass." IEEE Journal of Quantum Electronics, 11, 798-799, 1975.

Liao, P. F. and Weber, H. P. "Fluorescence Quenching of the  ${}^4F_{3/2}$  State in Nd-doped Yttrium Aluminum Garnet (YAG) by Multiphonon Relaxation." Journal of Applied Physics, 45, 2931-2934, July 1974.

Riseberg, L. A. and Moos, H. W. "Multiphonon Orbit-Lattice Relaxation of Excited States of Rare-Earth Ions in Crystals." Physical Review, 174, 429-438, October 1968.

Vasilev, I. V., et al. "Non-Resonance Excitation Energy Transfer Between Impurity Rare-Earth Ions." Soviet Physics-JETP, 29, 69-75, July 1969.

Weber, M. J. "Selective Excitation and Decay of  $Er^{+3}$  Fluorescence in  $LaF_3$ ." Physical Review, 156, 231-241, April 1967.

Weber, M. J. "Probabilities for Radiative and Non-Radiative Decay of  $Er^{+3}$  in  $LaF_3$ ." Physical Review, 157, 262-272, May 1967.

## VITA

Warren B. Maupin, II was born in Salina, Kansas on 21 September 1947, but spent the majority of his childhood in Texas. After graduating from high school in Dallas, Texas in 1965, he attended Texas A&M University graduating with a B. S. in chemical engineering in 1969. Following graduation, he was employed by Texas Instruments Inc. in Dallas until he entered Officer Training School in October 1969. He received his commission in December 1969 and was assigned to Mather AFB, California where he attended navigator training. Upon completion of navigator training in September 1970, he was assigned to the 50<sup>th</sup> Tactical Airlift Squadron at CCK AB, Taiwan where he served as a navigator on C-130 aircraft. In June 1972, he returned to Mather AFB to serve as an instructor in the navigator training program. While assigned at Mather, he married Virginia Lee Cochran of Bakersfield, California. He was assigned to the School of Engineering, Air Force Institute of Technology, in June 1975.

Permanent address: 212 Northwood MHP  
Lewisville, Texas 75067

REPORT DOCUMENTATION PAGE		READ INSTRUCTIONS BEFORE COMPLETING FORM
1. REPORT NUMBER GEP/PH/76-8	2. GOVT ACCESSION NO.	3. RECIPIENT'S CATALOG NUMBER
4. TITLE (and Subtitle) Output Power Variations in Nd:YAG Laser Hosts		5. TYPE OF REPORT & PERIOD COVERED MS Thesis
		6. PERFORMING ORG. REPORT NUMBER
7. AUTHOR(s)  Warren B. Maupin, II Captain		8. CONTRACT OR GRANT NUMBER(s)
9. PERFORMING ORGANIZATION NAME AND ADDRESS Air Force Institute of Technology (AFIT-EN) Wright-Patterson AFB, Ohio 45433		10. PROGRAM ELEMENT, PROJECT, TASK AREA & WORK UNIT NUMBERS
11. CONTROLLING OFFICE NAME AND ADDRESS		12. REPORT DATE December 1976
		13. NUMBER OF PAGES 62
14. MONITORING AGENCY NAME & ADDRESS (if different from Controlling Office)		15. SECURITY CLASS. (of this report) Unclassified
		15a. DECLASSIFICATION/DOWNGRADING SCHEDULE
16. DISTRIBUTION STATEMENT (of this Report)  Approved for public release; distribution unlimited		
17. DISTRIBUTION STATEMENT (of the abstract entered in Block 20, if different from Report)		
18. SUPPLEMENTARY NOTES  Approved for public release; IAW AFR 190-17 <i>Jerral F. Guess</i> JERRAL F. GUESS, Captain, USAF Director of Information		
19. KEY WORDS (Continue on reverse side if necessary and identify by block number) Neodymium Concentration Gradients Yttrium Aluminum Garnet Fluorescent Lifetime Cross Sections Solid State Lasers		
20. ABSTRACT (Continue on reverse side if necessary and identify by block number) Seemingly identical Nd:YAG laser rods often exhibit significant variations in output power. The purpose of this report is to investigate the possible cause or causes for the performance variations in Nd:YAG laser rods. The fundamental chemical and crystal growth characteristics of Nd:YAG are reviewed. The spectroscopy of Nd:YAG is discussed with emphasis on the laser transition. The more common spectroscopic parameters are defined and the important relationships		

SECURITY CLASSIFICATION OF THIS PAGE(When Data Entered)

between them derived. Expressions relating the laser performance of CW and Q-switched systems to the host parameters are developed and the important parameters ( $n$ ,  $\Delta v$ ,  $\tau_f$ ,  $\tau_{sp}$ ,  $\alpha$ ) are discussed. Possible energy transfer mechanisms to account for performance variations are presented and evaluated.

It is proposed that concentration variations are primarily responsible for laser performance fluctuations and a method for obtaining experimental verification is outlined.

SECURITY CLASSIFICATION OF THIS PAGE(When Data Entered)

DATE  
LME